

A Comparison of VN and NbN Thin Films Towards Optimal SNSPD Efficiency

Philipp Zolotov , Alexander Semenov, Alexander Divochiy, and Gregory Goltzman 

Abstract—Based on early phenomenological ideas about the operation of superconducting single-photon detectors (SSPD or SNSPD), it was expected that materials with a lower superconducting gap should perform better in the IR range. The plausibility of this concept could be checked using two popular SSPD materials - NbN and WSi films. However, these materials differ strongly in crystallographic structure (polycrystalline B1 *versus* amorphous), which makes their dependence on disorder different. In our work we present a study of the single-photon response of SSPDs made from two disordered B1 structure superconductors - vanadium nitride and niobium nitride thin films. We compare the intrinsic efficiency of devices made from films with different sheet resistance values. While both materials have a polycrystalline structure and comparable diffusion coefficient values, VN films show metallic behavior over a wide range of sheet resistance, in contrast to NbN films with an insulator-like temperature dependence of resistivity, which may be partially due to enhanced Coulomb interaction, leading to different starting points for the normal electron density of states. The results show that even though VN devices are more promising in terms of theoretical predictions, their optimal performance was not reached due to lower values of sheet resistance.

Index Terms—Superconducting photodetectors, superconductivity, thin films.

I. INTRODUCTION

MOVING towards middle IR range with superconducting single-photon detectors and their excellent performance at visible and near IR ranges remains an important and challenging task. As it was previously shown in references [1], [2] SSPDs have a potential of operation at wavelengths at least up to $5\ \mu\text{m}$ and at the moment are already used at $2.3\ \mu\text{m}$ [3] where other

single-photon detection technologies are practically unavailable. Taking into account the progress that was made during the last decade in the understanding of the main mechanisms responsible for photon detection in SSPDs [4]–[6], it is already possible to take further steps in increasing their performance at mid-IR. We demonstrated that the major impact on SSPD efficiency is made by sheet resistance of the films that are used for detector fabrication [7]. To verify if the sheet resistance increase work similarly for different superconducting thin-film materials with the same structure we test our approach with an alternative to conventional NbN material with the same B1 crystal structure - vanadium nitride (VN). It is expected that in accordance with the conventional model lower superconducting critical temperature T_c of VN films would result in a more efficient gap suppression in VN SSPDs at sub-eV photon energies [8]. In contrast to widely used tungsten silicide films, vanadium nitride has also a potential for operation in GM-based cryostats, which would significantly decrease the requirements for cryogenic setup.

II. SUPERCONDUCTING AND NORMAL-STATE PROPERTIES OF VANADIUM NITRIDE AND NIOBIUM NITRIDE THIN FILMS

A major influence of the superconducting gap value Δ over detecting process in SSPDs could be explained in the framework of “hotspot—vortex model” by Vodolazov *et al.* [4], [9]. The detection event could be separated into two interconnected stages. The first stage that is taking place after photon absorption is related to the appearing of a hotspot in the nanostrip biased with a supercurrent. The suppression of the order parameter in the spot will be mainly dependent on the number of quasiparticles created by an incident photon, which is given by the ratio between the energy of the photon and the gap: $h\nu/\Delta$. On the second stage, occurrence of the hotspot lowers the critical current of the cross section of the strip enabling its switch into resistive state if the supercurrent value is larger than the reduced nanostrip’s critical current. As we showed in the separate research [7], both Δ and this critical (detecting) current I_{det} are highly dependent on the sheet resistance R_s of the films. Therefore it is reasonable to use R_s as the main tuning parameter for device optimization and study of the evolution of device photoreponse with increasing disorder. Fig. 1 demonstrates the change in the detecting current normalized to the depairing current for two materials at variable R_s . As the model anticipates, at the same operating temperature and nanostrip width, the VN-based devices, indeed, have a more rapid drop of the normalized detecting current for increasing R_s than that of NbN-based devices. The estimation of the SSPD detecting current was conducted using the following

Manuscript received December 1, 2020; revised February 4, 2021; accepted February 7, 2021. Date of publication February 12, 2021; date of current version March 12, 2021. This work was supported by the Center of Excellence “Center of Photonics” funded by the Ministry of Science, and Higher Education of the Russian Federation under Contract 075-15-2020-906. (*Corresponding author:* Philipp Zolotov.)

Philipp Zolotov is with the School of Electronic Engineering, HSE Tikhonov Moscow Institute of Electronics and Mathematics, Moscow, Russia, and LLC Superconducting Nanotechnology (SCONTEL), Moscow, Russia, and also with Moscow Pedagogical State University, Moscow 119435, Russia (e-mail: fzolotov@hse.ru).

Alexander Semenov is with Moscow Pedagogical State University, Moscow 119435, Russia, and also with the Moscow Institute of Physics and Technology, Moscow 141701, Russia (e-mail: a_sem2@mail.ru).

Alexander Divochiy is with LLC Superconducting Nanotechnology (SCONTEL), Moscow 603950, Russia (e-mail: divochiy@scontel.ru).

Gregory Goltzman Divochiy is with the FRC Institute of Applied Physics RAS, Nizhny Novgorod 603950, Russia, and also with Moscow Pedagogical State University, Moscow 119435, Russia (e-mail: goltzman@rplab.ru).

Color versions of one or more figures in this article are available at <https://doi.org/10.1109/TASC.2021.3059230>.

Digital Object Identifier 10.1109/TASC.2021.3059230

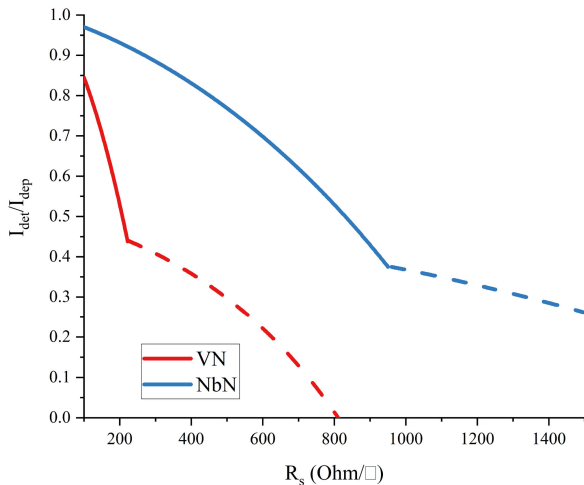


Fig. 1. The dependencies of the detecting current normalized to the depairing current for 100 nm NbN and VN strips at 1.7 K under luminescence of 1310 nm radiation. The curves are calculated using (1) (solid lines) and (2) (dashed lines).

expressions:

$$\frac{I_{det}}{I_{dep}} = 1 - \left[\frac{1}{2} + \frac{2D\tau}{w^2} \right] \times \frac{R_{b.t.}}{R_Q} \times \frac{N_{qp}}{4 \ln 2(kT_c\tau/\hbar)}, \quad (1)$$

$$\frac{I_{det}}{I_{dep}} = \frac{1}{2} - \frac{R_{b.t.}}{R_Q} \times \frac{\xi^2}{w^2} \times \frac{N_{qp}}{2 \ln 2}, \quad (2)$$

$$I_{dep}(T) = 0.74 \frac{w[\Delta(0)]^{3/2}}{eR_{b.t.}\sqrt{\hbar D}} \left[1 - \left(\frac{T}{T_c} \right)^2 \right]^{3/2}, \quad (3)$$

where N_{qp} is the number of quasiparticles in the hotspot, k - Boltzmann's constant, \hbar - Planck's constant divided by 2π , $R_{b.t.}$ is the normal-state sheet resistance as determined *before the transition* to superconducting state, I_{dep} - depairing current, $R_Q = 2\pi\hbar/(2e)^2$ is the quantum resistance, and $\xi = \sqrt{\hbar/kT_c}$. We used our experimental data from Fig. 2 to fit the relationship between sheet resistance and critical temperature for each material. This fitted relationships were used in 1 and 3 to obtain the dependencies from Fig. 1. For I_{dep} calculation in 3 operating temperature T was 1.7 K, and the diffusion coefficient D was constant and assumed to be 0.5 cm²/s, which is reasonable for both materials as shown in works [5], [9], [10]. 1 and 2 represent two scenarios, when the hotspot remains superconducting and when it becomes normal correspondingly. The expressions are based on the approach presented in [11] and are discussed in more detail in [7].

To test the photoresponse of actual devices we made two sets of film depositions with variable R_s values - one for each of the materials. While niobium nitride remains a well-known superconductor for several decades and multiple experimental works were dedicated to the optimization of its deposition techniques, VN remains much less explored superconducting nitride. Previously, we have shown that VN films remain superconducting up to the sheet resistance values of ~ 0.5 kOhm/□ [12]. Increasing the sheet resistance in VN films leads to a similar drop of T_c as was shown for other materials as well [13], [14]. These inherent relationships of $T_c(R_s)$ for VN and NbN thin films are presented in Fig. 2. It is important to highlight the difference in the behavior

of these two materials in terms of $R(T)$ curves also depicted in Fig. 2. Vanadium nitride, as it is expected from the Matthiessen rule, has a positive dR/dT value of the $R(T)$ curves in the normal state. The resistance of the films decreases at lower temperatures and then flows into a superconducting transition. The exception of this trend for VN is only highly-resistive films with dR/dT close to zero. In this case, the resistance of the films is expected to be dominated by impurity scattering even at close-to-room-temperatures. The niobium nitride, however, demonstrates unconventional behavior with $dR/dT < 0$. This phenomenon was recently highlighted in multiple works and is believed to be a part of so-called *marginal* superconductivity [15]. Taking into account the change in the sheet resistance of the films when compared at room temperature R_s^{film} and before the transition to the superconducting state $R_s^{film,b.t.}$ we took the latter values as normal state sheet resistance for calculations presented in this work.

III. INTRINSIC EFFICIENCY OF NBN AND VN SSPDs

NbN and VN films with different R_s values were used to fabricate SSPDs using a standard technological route for NbN films and a slightly modified route for VN films [12]. Due to the higher stability of the latter material to a reactive ion etching process in SF₆ and therefore longer film etching time we used different positive-tone resist to ensure the protection of sensitive element during fabrication of VN SSPDs. Other aspects of device fabrication and measurement techniques were the same for both materials under investigation. Deposited films in both sets had a similar thickness ranging from 4-8 nm measured with a quartz crystal. The variation of the sheet resistance was done by changing the deposition time and slight adjustment of the N₂ concentration in the gas mixture. Fabricated detectors had a conventional design - a 100 nm wide nanostrip folded as a meander with a total length of ~ 1 mm. The detectors were tested in a LHe dipstick at the operating temperature of 1.7 K. The detectors were coupled with a 1310 nm laser diode via single-mode fiber and an attenuator. In the framework of our study, we didn't attend to measure any absolute values of the quantum efficiency, focusing only on the intrinsic efficiency of the devices, i.e. probability of the detector to "click" after a photon was absorbed in its active element, regardless of the total photon flux. At the same time, the number of photocounts was kept below $\sim 1 \times 10^6$ counts/s to ensure a proper operation regime of the detectors [16].

Fig. 3 demonstrates the results of our experiments and Table I summarises the main parameters of the devices under investigation. The table contains the values of sheet resistance of the films and devices. For the films the values of sheet resistance are presented as for the room-temperature measurements R_s^{film} , as well as before the superconducting transition $R_s^{film,b.t.}$. To make sure that during the nanofabrication substantial film degradation did not take place, we also calculate the sheet resistance before the transition for devices $R_s^{dev,b.t.}$ by finding the number of squares in the nanostrip and dividing the resistance of the device before the transition to the superconducting state by this value. The table also contains the measured values of the critical temperature of the films T_c^{film} and calculated values

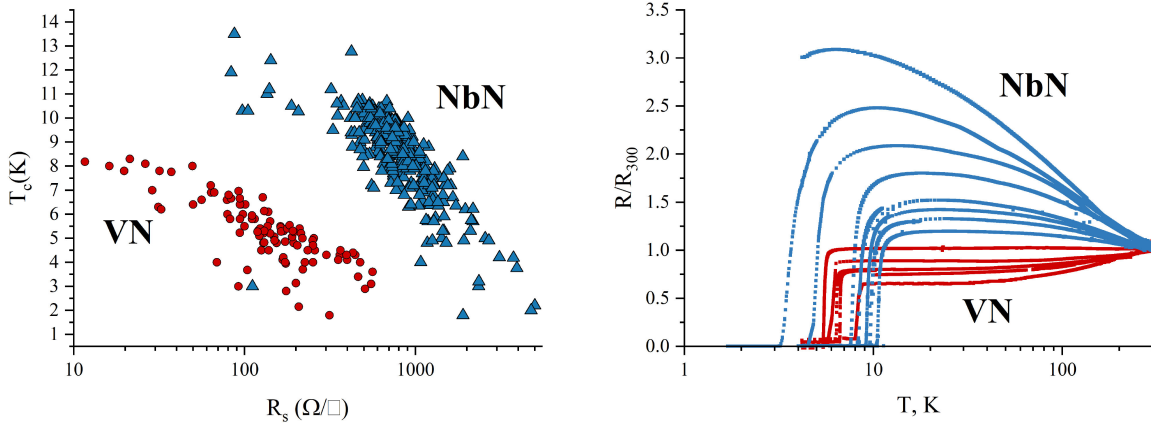


Fig. 2. Left graph: the relationship between sheet resistance and critical temperature of NbN and VN films deposited over the same substrate material. Right graph: resistance vs. temperature curves for two materials at variable R_s values.

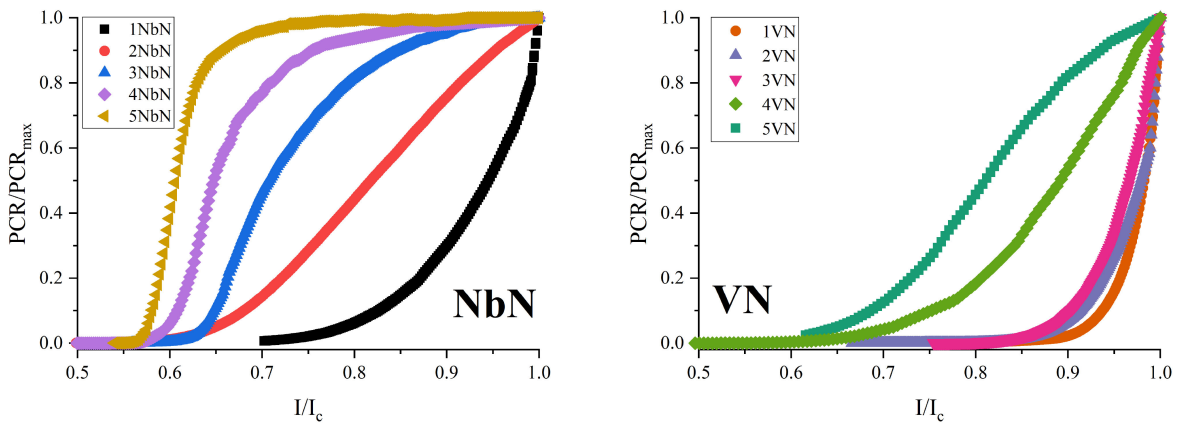


Fig. 3. The dependence of the photocount rate *vs.* normalized bias current for two materials and variable R_s values. Both materials demonstrate the change of the intrinsic detection efficiency on a three-fold scale of $R_s^{dev.b.t.}$ values presented in Table I.

TABLE I
MAIN PARAMETERS OF STUDIED DEVICES

#	R_s^{film} , Ω/\square	$R_s^{film\ b.t.}$, Ω/\square	T_c^{film} , K	$R_s^{dev.b.t.}$, Ω/\square	$T_c^{dev.fit}$, K
1NbN	282	340	11.4	396	10.5
2NbN	350	479	9.7	439	10.3
3NbN	490	721	9.5	782	9
4NbN	556	830	9.2	871	8.7
5NbN	650	867	9.3	1083	8.1
1VN	147	126	6	67	6.2
2VN	115	97	6.4	109	5.6
3VN	165	154	4.7	146	5.1
4VN	202	176	5.5	178	4.9
5VN	202	173	5.5	190	4.8

of the critical temperature of the devices using their $R_s^{dev.b.t.}$ and fitting functions of the plots from Fig. 2. For both materials $R_s^{dev.b.t.}$ has a three-fold change with different starting points. For NbN detectors the saturation drops from the pronounced unity value for the device 5NbN with the highest $R_s^{dev.b.t.}$ down to the values below half-unity for 1NbN with the lowest sheet resistance before the transition. The most resistive VN device 5VN shows much less pronounced saturation compared to 5NbN with ~ 0.9 from unity intrinsic efficiency. Given the fact that

both film sets had a similar range of thicknesses, we link such a difference with the density of states that relates to the sheet resistance as $e^2 N_{2D} D = 1/R_s$. With a clear trend to saturated quantum efficiency curve for higher sheet resistance values for both materials, we conclude that more resistive films are more suitable for high-efficiency SSPD fabrication regardless of the material bulk Δ value.

IV. CONCLUSION

Investigation of the SSPDs operation using different superconducting materials is a crucial piece of information required to better understand the physics behind these devices. In our work, from a comparison of two B1 superconducting thin-film materials, we conclude that disorder represented in the films with their sheet resistance plays a crucial role in photoresponse. By increasing the sheet resistance of the films as measured before the transition to the superconducting state it is possible to enhance the photoresponse of the SSPDs and move towards the mid-IR range without sacrificing the detection efficiency.

ACKNOWLEDGMENT

The authors would like to thank T. M. Klapwijk for his advisement in results analysis.

REFERENCES

- [1] L. Maingault *et al.*, "Spectral dependency of superconducting single photon detectors," *J. Appl. Phys.*, vol. 107, no. 9, 2010, Art. no. 116103.
- [2] F. Marsili *et al.*, "Efficient single photon detection from 500 nm to 5 μm wavelength," *Nano Lett.*, vol. 12, no. 9, pp. 4799–4804, 2012.
- [3] A. Divochiy *et al.*, "Single photon detection system for visible and infrared spectrum range," *Opt. Lett.*, vol. 43, no. 24, pp. 6085–6088, 2018.
- [4] D. Y. Vodolazov, "Single-photon detection by a dirty current-carrying superconducting strip based on the kinetic-equation approach," *Phys. Rev. Appl.*, vol. 7, no. 3, 2017, Art. no. 034014.
- [5] Y. P. Korneeva *et al.*, "Optical single-photon detection in micrometer-scale nbn bridges," *Phys. Rev. Appl.*, vol. 9, no. 6, 2018, Art. no. 064037.
- [6] D. V. Reddy, R. R. Nerem, S. W. Nam, R. P. Mirin, and V. B. Verma, "Superconducting nanowire single-photon detectors with 98% system detection efficiency at 1550 nm," *Optica*, vol. 7, no. 12, pp. 1649–1653, 2020.
- [7] P. I. Zolotov, A. V. Semenov, A. V. Divochiy, G. N. Goltsman, N. R. Romanov, and T. M. Klapwijk, "Dependence of photon detection efficiency on normal-state sheet resistance in marginally superconducting films of NbN," *IEEE Trans. Appl. Supercond.*, vol. 31, no. 5, pp. 279–302, 2021.
- [8] A. Engel *et al.*, "Tantalum nitride superconducting single-photon detectors with low cut-off energy," *Appl. Phys. Lett.*, vol. 100, no. 6, 2012, Art. no. 062601.
- [9] A. Korneev, A. Semenov, D. Vodolazov, G. N. Gol'tsman, and R. Sobolewski, *Superconductors At the Nanoscale: From Basic Research to Applications*, vol. 9, 1st Ed. De Gruyter, 2017.
- [10] N. Romanov, P. Zolotov, Y. B. Vakhtomin, A. Divochiy, and K. Smirnov, "Electron diffusivity measurements of VN superconducting single-photon detectors," in *Proc. J. Phys.: Conf. Ser.*, vol. 1124, no. 5, 2018, Art. no. 051032.
- [11] A. Zotova and D. Y. Vodolazov, "Photon detection by current-carrying superconducting film: A time-dependent Ginzburg-Landau approach," *Phys. Rev. B*, vol. 85, no. 2, 2012, Art. no. 024509.
- [12] P. Zolotov *et al.*, "Influence of sputtering parameters on the main characteristics of ultra-thin vanadium nitride films," in *Proc. J. Phys.: Conf. Ser.*, vol. 1124, no. 5, 2018, Art. no. 051030.
- [13] A. Finkel'Stein, "Suppression of superconductivity in homogeneously disordered systems," *Physica B: Condens. Matter*, vol. 197, no. 1-4, pp. 636–648, 1994.
- [14] Y. Ivry *et al.*, "Universal scaling of the critical temperature for thin films near the superconducting-to-insulating transition," *Phys. Rev. B*, vol. 90, no. 21, 2014, Art. no. 214515.
- [15] B. Sacépé, M. Feigel'man, and T. M. Klapwijk, "Quantum breakdown of superconductivity in low-dimensional materials," *Nat. Phys.*, vol. 16, no. 7, pp. 734–746, 2020.
- [16] A. J. Kerman *et al.*, "Kinetic-inductance-limited reset time of superconducting nanowire photon counters," *Appl. Phys. Lett.*, vol. 88, no. 11, 2006, Art. no. 111116.